Force/Torque-Sensorless Joint Stiffness Estimation in Articulated Soft Robots

Maja Trumić[1], Giorgio Grioli[2], Kosta Jovanović[3], and Adriano Fagiolini[4]

***Abstract*—Currently, the access to the knowledge of stiffness values is typically constrained to a-priori identified models or datasheet information, which either do not usually take into account the full range of possible stiffness values or need extensive experiments. This work tackles the challenge of stiffness estimation in articulated soft manipulators, and it proposes an innovative solution adding value to the previous research by removing the necessity for force/torque sensors and generalizing to multi-degree-of-freedom robots. Built upon the theory of unknown input-state observers and recursive least-square algorithms, the solution is independent of the actuator model parameters and its internal control signals. The validity of the approach is proven analytically for single and multiple degree-of-freedom robots. The obtained estimators are first evaluated via simulations on articulated soft robots with different actuations and then tested in experiments with real robotic setups using antagonistic variable stiffness actuators.**

***Index Terms*—Calibration and Identification, Compliant Joints and Mechanisms, Flexible Robots, Safety in HRI**

I. Introduction

THERE is a growing interest in exploiting the full potential of articulated soft robots, i.e. vertebrate-inspired systems consisting of rigid links interconnected by compliant joints [1]. However, to fully let these robots reach the edge with respect to their rigid counterparts, both in terms of performance and safe human-robot interaction, consistent and accurate knowledge of joint stiffness is paramount, which is a challenge for the fact that stiffness itself is not measurable [2]. A common practice for stiffness assessment is to rely on mathematical models, experimentally determined prior to the robot utilization. Some manufacturers of joint actuators provide this information in the form of a function of the internal configuration of the actuation device. However, the provided model can only describe a nominal characterization of the joint stiffness, which in fact depends on the device temperature and whose accuracy degrades with the increase of the elastic elements' wear [3], thus possibly leading to unacceptable performance loss and safety degradation. Moreover, if such a model is unavailable, an articulated-robot designer has to spend considerable time for its identification, which may involve understanding which nonlinearities can be neglected so as to trade between model complexity and accuracy.

This limitation is now motivating the shift toward the adoption of online and adaptive stiffness estimators. Along this line, the problem of estimating stiffness in the Cartesian space has been tackled in [4] for robots in contact with the environment. Successive works have successfully addressed the estimation problem in the joint space both from the so-called motor side [5]–[8] and link side [9], [10], which is crucial for ensuring the safety of humans who can collide with the robot sideways. With regard to these methods, full motor-side approaches avoid using information about the robot dynamics but require knowledge of the actuation device motor controls (in terms of torques or currents) for which they are considered *invasive* solutions. Contrarily, a link-side solution such as in [9] uses information about the robot kinematics, dynamics, and external forces, and is thus regarded as *noninvasive*, but tend to suffer from observability issues. Interestingly, according to recent trends in rehabilitation robotics, link-side stiffness approaches are believed to become advantageous for parameter estimation in human-robot cooperation [11], as well as for assessing human stiffness during teleoperation [12]. Concerning this last perspective, they also avoid the need to install sensors in the human body. Yet, all the aforementioned approaches rely on the availability of force/torque sensor data, whose placement is often impractical or even impossible due to its invasiveness, as well as more expensive. Also, link-side solutions have considered stiffness estimation for a single degree-of-freedom (DoF) structure only.

To overcome current limitations and simplify the usage of stiffness estimators in various spheres of robotics, the present work addresses the problem of joint stiffness estimation with *force/torque sensorless* techniques. We consider here the joint stiffness that is the passive, or internal, stiffness of a robot joint, indicating the amount of joint torque change that is necessary to produce a deformation of the joint's elastic transmission from the current value. Joint torque is, in turn, the elastic torque transferred from the actuator motors to the robot link via elastic transmission. The letter proposes an innovative solution that can be viewed as *semi-invasive* for needing only the motor positions and speeds of the used actuators, but being independent of their dynamic models and internal controls. Specifically, the independence from the actuation control commands is obtained by suitably decoupling the reconstruction of the elastic torque time-derivative via a delayed Unknown Input-state Observer (UIO) [13]. In this respect, a first theoretical contribution of this letter is to show how the joint stiffness estimation can be resolved into that of the elastic rotatum p_e, which in turn is possible by using UIO theory provided that the robot's dynamic model is suitably reformulated. Moreover, by presenting a general way

Manuscript received: January 20, 2022; Revised April, 13, 2022; Accepted May, 12, 2022.

This paper was recommended for publication by Editor Lucia Pallottino upon evaluation of the Associate Editor and Reviewers' comments. This research has partly received funding from the EU's ERC programme under the Grant Agreement No. 810346 (Natural Bionics) and by the Science Fund of the Republic of Serbia, PROMIS, #6062528, ForNextCobot.

[1]Maja Trumić is with the School of Electrical Engineering, University of Belgrade, Serbia and with the Mobile & Intelligent Robots @ Panormous Laboratory (MIRPALab), Department of Engineering, University of Palermo, 90128, Palermo, Italy, maja.trumic@etf.rs.

[2]Giorgio Grioli is with the Italian Institute of Technology, Genoa, Italy, and with Centro di Ricerca "E. Piaggio" of the University of Pisa, Pisa, Italy, giorgio.grioli@iit.it.

[3]Kosta Jovanović is with the School of Electrical Engineering, University of Belgrade, Serbia, kostaj@etf.rs.

[4]Adriano Fagiolini is with the Mobile & Intelligent Robots @ Panormous Laboratory (MIRPALab), Department of Engineering, University of Palermo, 90128, Palermo, Italy fagiolini@unipa.it.

Digital Object Identifier (DOI): see top of this page.

to factorize each VSA model as the product of a regressor matrix and a coefficient vector, the letter presents an instrumental connection between elastic rotatum and joint stiffness, which is a crucial enabler for applying Recursive Least-Square (RLS)-based learning [14] that allows extracting the sought stiffness signal and achieving independence from the actuation model. Lastly, capitalizing on the decentralized nature of the elastic torque time-derivative, a third theoretical contribution of the letter is an analytical proof that n identical copies of a universal 1-DoF stiffness estimator can be used.

The letter contributes to the state-of-the-art by presenting an innovative solution with the following advantages: 1) In a broad manner, it substantially reduces cost and complexity by avoiding the installation and calibration of force/torque sensors, a choice recently advocated in works such as [15]; 2) it presents a *semi-invasive*, link-side stiffness estimator for n-joint articulated soft robots; 3) it offers a unifying framework that extends to the wide range of compliant actuators: Series Elastic Actuators (SEA) [16], serial Variable Stiffness Actuators (sVSA) (e.g. AwAS [17], SVSA-II [18], vsaUT-II [19]) and antagonistic Variable Stiffness Actuators (aVSA) (e.g. VSA-HD [20], QA-Joint [21], qbmove [22]); 4) it does not need link speed and acceleration at the only expense of a few sample delays [13]. The proposed estimator is validated in simulation, by applying it to three robots with different types of actuators, and then through experimental tests on real robot setups with different configurations.

II. System Model and Problem Statement

Consider an n-DoF articulated soft robot consisting of n pairs of rigid links and elastically-decoupled flexible joints. Assuming a negligible inertia coupling between motors and joints and link-position dependent gravity potential and mass matrix, the robot's dynamic model reads [2]:

$$\begin{aligned} M(q)\,\ddot{q} + C(q,\dot{q})\,\dot{q} + G(q) + \gamma(\dot{q}) + \tfrac{\partial V(q,\theta)^T}{\partial q} &= \tau_{\text{ext}}\,, \\ B\,\ddot{\theta} + D\,\dot{\theta} + \tfrac{\partial V(q,\theta)^T}{\partial \theta} &= \tau\,, \end{aligned} \tag{1}$$

where $q = (q_1, \cdots, q_n)^T$ is the link position vector, $\theta = (\theta_1, \cdots, \theta_m)^T$ is the motor position vector, $M(q)$ is the robot inertia matrix, $C(q,\dot{q})$ is a matrix formed of Coriolis and centrifugal terms, $G(q)$ is the gravity vector, $\gamma(\dot{q})$ is a vector comprising static and viscous friction terms, $V(q,\theta)$ is the elastic potential energy, τ_{ext} is an external torque, $B = \text{diag}(\text{b}_1, \cdots, \text{b}_\text{n})$ is the motor inertia matrix, and $D = \text{diag}(\text{d}_1, \cdots, \text{d}_\text{n})$ is the motor damping matrix, and, finally, $\tau = (\tau_1, \cdots, \tau_n)^T$ is the actuator input torque vector. This model is broad enough to accommodate the description of a wide range of articulated soft robots. Three different instances of the proposed model are considered in this letter:

1) *SEA-driven robots*. The constant elasticity of these robots' joints arises from the linear spring that connects in series a single, directly-actuated motor and a robot joint. They have a negligible stiffness adjusting mechanism and, hence, their potential energy reduces to $V(\phi) = \frac{1}{2}\phi^T K \phi$, where $K \in \mathbb{R}^{n,n}$ is a diagonal matrix, whose i-th entry is the i-th actuator spring constant, and $\phi = q - \theta$ is the transmission deflection vector with $q, \theta \in \mathbb{R}^n$. The elastic torque vector and joint stiffness matrix become consequently $\tau_e(\phi) = \frac{\partial V(\phi)^T}{\partial \phi} = K\phi\,,\ \sigma(\phi) = \frac{\partial \tau_e(\phi)}{\partial \phi} = K\,.$ Since $\frac{\partial V(q,\theta)}{\partial q} = -\frac{\partial V(q,\theta)}{\partial \theta} = \frac{\partial V(\phi)}{\partial \phi}$, a SEA-driven robot's dynamics can be written in the form

$$\begin{aligned} M(q)\,\ddot{q} + C(q,\dot{q})\,\dot{q} + G(q) + \gamma(\dot{q}) + \tau_e(\phi) &= \tau_{\text{ext}}\,, \\ B\,\ddot{\theta} + D\,\dot{\theta} - \tau_e(\phi) &= \tau\,. \end{aligned} \tag{2}$$

2) *Serial VSA-driven robots*. Besides having a motor that directly sets the link position, these robots are equipped with the stiffness adjusting mechanism that allows online and independent setting of both position and stiffness. Thus, their potential energy is $V(q,\theta) = V(\theta_c, \phi) = V_{\theta_c}(\theta_c)\, V_\phi(\phi)$, where $\phi = q - \theta_a$, with $\theta_a \in \mathbb{R}^n$ being the configuration of a first motor, which determines the link position, and $\theta_c \in \mathbb{R}^n$ configuration of a second motor, that adjusts stiffness. Again, considering that $\frac{\partial V(q,\theta)}{\partial q} = -\frac{\partial V(q,\theta)}{\partial \theta_a} = \frac{\partial V(\theta_c,\phi)}{\partial \phi}$, their dynamics reads

$$\begin{aligned} M(q)\,\ddot{q} + C(q,\dot{q})\,\dot{q} + G(q) + \gamma(\dot{q}) + \tau_e(\theta_c,\phi) &= \tau_{\text{ext}}\,, \\ B_a\,\ddot{\theta}_a + D_a\,\dot{\theta}_a - \tau_e(\theta_c,\phi) &= \tau_a\,, \\ B_c\,\ddot{\theta}_c + D_c\,\dot{\theta}_c + \psi_e(\theta_c,\phi) &= \tau_b\,, \end{aligned} \tag{3}$$

where the elastic torque, the coupling elastic torque, and the joint stiffness matrix $\sigma \in \mathbb{R}^{n,n}$ are

$$\tau_e = \tfrac{\partial V(\theta_c,\phi)^T}{\partial \phi},\ \psi_e = \tfrac{\partial V(\theta_c,\phi)^T}{\partial \theta_c},\ \sigma = \tfrac{\partial \tau_e(\theta_c,\phi)}{\partial \phi}\,,$$

with σ being a diagonal matrix due to the joints' elastic decoupling. The independence of the motor roles, for every i-th joint, let the expression of the elastic torque be factorized as $\tau_{e_i} = \tau^{\theta_c}_{e_i}(\theta_{c_i})\, \tau^{\phi}_{e_i}(\phi_i)$ [23].

3) *Agonistic-Antagonistic VSA-driven robots*. Their main advantage stems in the nonlinear antagonistic coupling between two motors and the joint, allowing simultaneous position and stiffness setting. According to [8], their potential energy satisfies the condition $V(q,\theta) = \sum_j V(\phi_j)$, with $\phi_j = q - \theta_j$ where $j = a, b$ indicates the agonistic and antagonistic motors, which induces the relation $\frac{\partial V(q,\theta)}{\partial q} = -\sum_j \frac{\partial V(q,\theta_j)}{\partial \theta_j} = \sum_j \frac{\partial V(\phi_j)}{\partial \phi_j}$, and their dynamics is

$$\begin{aligned} &M(q)\,\ddot{q} + C(q,\dot{q})\,\dot{q} + G(q) + \gamma(\dot{q}) + \tau_{e_a}(\phi_a) + \tau_{e_b}(\phi_b) = \tau_{\text{ext}}\,, \\ &B_a\,\ddot{\theta}_a + D_a\,\dot{\theta}_a - \tau_{e_a}(\phi_a) = \tau_a,\ B_b\,\ddot{\theta}_b + D_b\,\dot{\theta}_b - \tau_{e_b}(\phi_b) = \tau_b\,, \end{aligned} \tag{4}$$

with $q, \theta_a, \theta_b \in \mathbb{R}^n$, $\tau_{e_j}(\phi_j) = \frac{\partial V(\phi_j)^T}{\partial \phi_j}$ and $\sigma_j(\phi_j) = \frac{\partial \tau_{e_j}(\phi_j)}{\partial \phi_j}$ being the local elastic torque and local diagonal stiffness matrix, so the total stiffness matrix is $\sigma = \sum_j \sigma_j$.

Assuming for simplicity that the external torque and friction are null, $\tau_{\text{ext}} = 0, \gamma(\dot{q}) = 0$, and recalling that stiffness is not measurable, this letter addresses the following:

Problem 1 (Joint Stiffness Estimation): Given an articulated soft robot as in (1), find a *force/torque-sensorless* estimation strategy of the joint stiffness matrix $\sigma = \text{diag}(\sigma_1, \cdots, \sigma_\text{n})$, using only motor state information, link positions and dynamics. Implicitly, the sought solution is required to be independent of the commanded motor torque τ.

III. Stiffness Estimation

A. Mathematical Framework of delayed UIOs

Consider a discrete-time linear system of the form

$$X_{k+1} = \bar{A}\,X_k + \bar{B}\,U_k\,, \quad Y_k = \bar{C}\,X_k + \bar{D}\,U_k\,, \tag{5}$$

where $X_k \in \mathbb{R}^{\bar{n}}$ is a state vector, $U_k \in \mathbb{R}^{\bar{m}}$ is an unknown input vector, $Y_k \in \mathbb{R}^p$ is an output vector. If $(\bar{B}^T, \bar{D}^T)^T$ is full-column rank, the following holds [13]:

Proposition 1 (Delayed Unknown-Input Observer): Given a system as in (5) and a delay $L \in \mathbb{N}^+$, the discrete-time linear system

$$\hat{X}_{k+1} = E\,\hat{X}_k + F\,\mathbb{Y}^L_k\,,\ \hat{U}_k = \mathcal{J}\begin{pmatrix} \hat{X}_{k+1} - \bar{A}\,\hat{X}_k \\ Y_k - \bar{C}\,\hat{X}_k \end{pmatrix}\,, \tag{6}$$

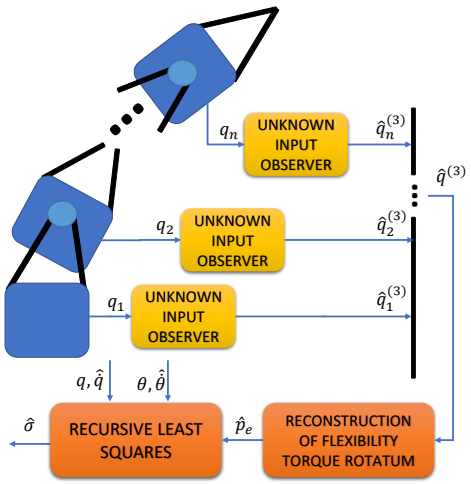

Fig. 1. Block diagram depiction of the semi-invasive stiffness estimator for flexible robot joints, actuated by electromechanical actuators. The solution comprises n identical copies of a 1-DoF UIO estimator and n identical copies of a 1-DoF RLS filter.

where $\mathbb{Y}_k^L = \left(Y_{k-L}^T, \cdots, Y_k^T\right)^T$ is the system output history recorded over $L+1$ time samples, $\mathcal{J}$ is the left-pseudoinverse of $(\bar{B}^T, \bar{D}^T)^T$, and E and F satisfy the conditions:

A1) $F\,\mathbb{H}^L = (\bar{B}, 0_{\bar{n},\bar{m}})$ (*input decoupling*),
A2) $E = \bar{A} - F\,\mathbb{O}^L$ (*initial state decoupling*),
A3) E is Schur, i.e. all its eigenvalues are within the unit circle (*free solution convergence*),

where $\mathbb{H}^L$ and $\mathbb{O}^L$ are the L-step invertibility and observability matrices, can generate state and input estimates, $\hat{X}_k \in \mathbb{R}^{\bar{n}}$ and $\hat{U}_k \in \mathbb{R}^{\bar{m}}$, asymptotically tracking the real ones, i.e. $\lim_{k\to\infty}(\hat{X}_k - X_k) = 0\,,\ \lim_{k\to\infty}(\hat{U}_k - U_k) = 0.$ □

A system as in (6) allows estimating the system state regardless of the unknown input U_k with a delay L. The choice of L is not heuristic, yet system dependent, thus it is a-priorly calculated to meet the system's invertibility and strong observability properties (5) [13].

B. Joint Stiffness Estimation in Articulated Soft Robots

The estimator for online joint stiffness reconstruction in n-DoF robots as in (1) is described here. Referring to Fig. 1, the solution comprises a UIO, computing an estimate of the elastic rotatum vector $p_e[k] = (p_{e_1}[k], \cdots, p_{e_n}[k])^T$, i.e. the time derivative of the elastic torque vector, and an RLS filter, retrieving the entries of the joint stiffness matrix, $\hat{\sigma} = \mathrm{diag}(\hat{\sigma}_1, \cdots, \hat{\sigma}_n)$; the RLS filter initially learns the coefficients of a polynomial approximation of σ. Noticeably, the estimator has a *decentralized* form consisting of n copies of a 1-DoF UIO and of 1-DoF RLS filter, both using i-th joint and actuator data only: the i-th joint position $q_i[k]$ is the only input to the i-th UIO, and the estimated i-th joint speed $\hat{q}_i[k]$, and the i-th motor states are the inputs to the i-th RLS filter. The involved components are presented below.

1) Elastic rotatum vector estimation: The derivation of this component leverages on the decentralized nature of the elastic potential energy V, which induces two useful properties: a) $\frac{\partial V(q_i,\theta)}{\partial q_j} = 0$ for all $i \neq j$; b) the i-th elastic rotatum, i.e. the first time derivative of V's partial derivative in q, is $p_{e_i} = \frac{d}{dt}\frac{\partial V(q_i,\theta)}{\partial q_i}$ and hence it contains information about the i-th joint stiffness [5]. The explicit formulas following from the latter property are reported in Table I for the three actuation principles. Then, the following main result can be stated:

SEA	$p_{e_i} = \dot{\tau}_{e_i} = \frac{d}{dt}\left(\frac{\partial V(q_i,\theta_i)}{\partial q_i}\right) = \frac{d}{dt}\left(\frac{\partial V(\phi_i)}{\partial \phi_i}\right) = \frac{\partial \tau_{e_i}}{\partial \phi_i}\dot{\phi}_i = \sigma_i \dot{\phi}_i$
sVSA	$p_{e_i} = \dot{\tau}_{e_i} = \frac{d}{dt}\left(\frac{\partial V(q_i,\theta_i)}{\partial q_i}\right) = \frac{d}{dt}\left(\frac{\partial V(\theta_{c_i},\phi_i)}{\partial \phi_i}\right) = = \frac{\partial \tau_{e_i}}{\partial \phi_i}\dot{\phi}_i + \frac{\partial \tau_{e_i}}{\partial \theta_{c_i}}\dot{\theta}_{c_i} = \sigma_i \dot{\phi}_i + \frac{\partial \tau_{e_i}}{\partial \theta_{c_i}}\dot{\theta}_{c_i}$
aVSA	$p_{e_i} = \dot{\tau}_{e_i} = \frac{d}{dt}\left(\frac{\partial V(q_i,\theta_i)}{\partial q_i}\right) = \frac{d}{dt}\left(\frac{\partial V(\phi_{a_i})}{\partial \phi_{a_i}} + \frac{\partial V(\phi_{b_i})}{\partial \phi_{b_i}}\right) = = \frac{\partial \tau_{e_{a_i}}}{\partial \phi_{a_i}}\dot{\phi}_{a_i} + \frac{\partial \tau_{e_{b_i}}}{\partial \phi_{b_i}}\dot{\phi}_{b_i} = \sigma_{a_i}\dot{\phi}_{a_i} + \sigma_{b_i}\dot{\phi}_{b_i}$

TABLE I
EXPLICIT RELATION BETWEEN THE ELASTIC ROTATUM p_{e_i} AND JOINT STIFFNESS σ_i FOR EACH ACTUATION PRINCIPLE.

Theorem 1 (Elastic Rotatum Vector Estimator): Given a sampling period T, the discrete-time linear system

$$\hat{X}_{k+1} = E\,\hat{X}_k + F\,\mathbb{Y}_k,\ \hat{U}_k = \mathcal{J}\begin{pmatrix}\hat{X}_{k+1} - A_n\hat{X}_k \\ q[k] - \hat{q}[k]\end{pmatrix}, \tag{7}$$

with $\mathbb{Y}_k = (q[k-3]^T, q[k-2]^T, q[k-1]^T, q[k]^T)^T$, $\hat{X}_k = (\hat{q}[k]^T, \hat{\dot{q}}[k]^T, \hat{\ddot{q}}[k]^T)^T$, and

$$E = \begin{pmatrix} \mathbb{I}_n & T\,\mathbb{I}_n & 0_n \\ 0_n & \mathbb{I}_n & T\,\mathbb{I}_n \\ -\mathbb{I}_n/T^2 & -3\mathbb{I}_n/T & -2\,\mathbb{I}_n \end{pmatrix},\ A_n = \begin{pmatrix} \mathbb{I}_n & T\,\mathbb{I}_n & 0_n \\ 0_n & \mathbb{I}_n & T\,\mathbb{I}_n \\ 0_n & 0_n & \mathbb{I}_n \end{pmatrix},$$
$$F = \begin{pmatrix} 0_{2n,3n} & 0_{2n,n} \\ 0_{n,3n} & \mathbb{I}_n/T^2 \end{pmatrix},\ \mathcal{J} = (0_{n,2n} \quad \mathbb{I}_n/T \quad 0_n)\,, \tag{8}$$

estimates in finite time the elastic rotatum vector as

$$\begin{aligned}\hat{p}_e[k] \;=\; & -M(\hat{q}[k])\,\hat{U}_k - \dot{M}(q[k],\hat{\dot{q}}[k])\,\hat{\dot{q}}[k] + \\ & - \dot{C}(q[k],\hat{\dot{q}}[k])\,\hat{\dot{q}}[k] - C(\hat{q}[k],\hat{\dot{q}}[k])\,\hat{\ddot{q}}[k] - \dot{G}(q[k],\hat{\dot{q}}[k])\,.\end{aligned} \tag{9}$$

Proof 1: To connect the stiffness to the link dynamics, one can differentiate the first equation of (1) as follows:

$$M q^{(3)} + \dot{M}\ddot{q} + \dot{C}\dot{q} + C\ddot{q} + \dot{G} + p_e = 0\,, \tag{10}$$

and left-multiply both members of the obtained expression by M^{-1} and lump all nonlinear terms into a virtual input

$$U = -M^{-1}\left(p_e + \dot{M}\ddot{q} + \dot{C}\dot{q} + C\ddot{q} + \dot{G}\right), \tag{11}$$

which yields $q^{(3)} = U$, that in state form is $\dot{X} = A_c\,X + B_c\,U$, $q = \bar{C}\,X + \bar{D}\,U$, with $X = (q^T, \dot{q}^T, \ddot{q}^T)^T$ and

$$A_c = \begin{pmatrix} 0_n & \mathbb{I}_n & 0_n \\ 0_n & 0_n & \mathbb{I}_n \\ 0_n & 0_n & 0_n \end{pmatrix},\ B_c = \begin{pmatrix} 0_n \\ 0_n \\ \mathbb{I}_n \end{pmatrix},\ \begin{matrix}\bar{C} = (\mathbb{I}_n\ 0_n\ 0_n)\,, \\ \bar{D} = 0_n\end{matrix}.$$

Time-discretizing the above model according to Euler's rule with the sampling period T and defining the discrete-time signals $X_k = X(kT)$, $U_k = U(kT)$, $q[k] = q(kT)$, where k is a time-step, leads to $X_{k+1} = A_n\,X_k + \bar{B}\,U_k$, $q[k] = \bar{C}\,X_k + \bar{D}\,U_k$, with A_n as in (8) and $\bar{B} = TB_c = (0_n, 0_n, T\,\mathbb{I}_n)^T$. The above matrices A_n, $\bar{B}$, $\bar{C}$, and $\bar{D}$ can be referred to the generic system in (5) with $\bar{n} = 3n$ and $\bar{m} = n$; also, they satisfy the invertibility condition with a delay $L = 3$, which ensures the feasibility of the UIO construction when the output history $\mathbb{Y}_k$ is as in the theorem's statement, i.e. comprising 4 consecutive samples of the link position $q[k]$. Direct computation of the 3-step invertibility and observability matrices defined in [13] gives

$$\mathbb{H}^3 = \begin{pmatrix} 0_{3n,n} & 0_{3n,3n} \\ T^3\mathbb{I}_n & 0_{n,3n} \end{pmatrix},\ \mathbb{O}^3 = \begin{pmatrix} \mathbb{I}_n & 0_n & 0_n \\ \mathbb{I}_n & T\mathbb{I}_n & 0_n \\ \mathbb{I}_n & 2T\mathbb{I}_n & T^2\mathbb{I}_n \\ \mathbb{I}_n & 3T\mathbb{I}_n & 3T^2\mathbb{I}_n \end{pmatrix}. \tag{12}$$

The procedure to derive the rotatum estimator involves satisfying the conditions of Prop. 1. Specifically, A1) for

an n-DoF system is $F\mathbb{H}^3 = (\bar{B}, 0_{3n,n})$. A convenient way to solve it is finding $F = \hat{F}N$ with N so that $N\,\mathbb{H}^3 = \begin{pmatrix} 0_{3n,n} & 0_{3n,3n} \\ \mathbb{I}_n & 0_{n,3n} \end{pmatrix}$. Direct inspection reveals that $N = \mathrm{diag}\left(\mathbb{I}_{3n}, \frac{1}{\mathrm{T}^3}\mathbb{I}_n\right)$ is a solution. Now, $F\mathbb{H}^3$ is rewritten as $\hat{F}N\mathbb{H}^3 = \hat{F}\begin{pmatrix} 0_{3n,n} & 0_{3n,3n} \\ \mathbb{I}_n & 0_{n,3n} \end{pmatrix} = (\bar{B}, 0_{3n,n})$. By partitioning $\hat{F}$ in accordance with the right-hand side of the above relation, i.e. as $\hat{F} = (\hat{F}_1, \hat{F}_2)$ yields the condition $\hat{F}_1\, 0_{3n,n} + \hat{F}_2\, \mathbb{I}_n = \bar{B}$ and hence $\hat{F}_2 = (0_n, 0_n, T\,\mathbb{I}_n)^T$, with undetermined $\hat{F}_1$, which plugged into F satisfies A1). Then, according to A2), it must hold $E = A_n - (\hat{F}_1, \bar{B})\, N\, \mathbb{O}^3$, where $\hat{F}_1$ can be used to make E Schur and thus, also satisfy A3). It is direct to check that the choice $\hat{F}_1 = 0_{3n}$ leads to the matrices E and F in (8). Lastly, choosing $\mathcal{J}$ as the left-pseudoinverse of $(\bar{B}^T, \bar{D}^T)^T$ leads to (8). Finally, solving (11) for p_e and replacing in it the continuous-time quantities with the sampled measure $q[k]$ and the UIO estimates, $\hat{q}[k]$, $\hat{\dot{q}}[k]$, $\hat{\ddot{q}}[k]$ and $\hat{U}_k$, gives the elastic rotatum formula in (9).

Moreover, inspection of the UIO matrices suggests that p_e can be computed via n independent copies of 1-DoF UIO. Appealingly, this implies that the solution scales with n, and indeed that, for an n-DoF soft robot, it suffices to realize n copies of the same 1-DoF UIO, as it is shown below:

Corollary 1 (Decentralized UIO): Under the hypotheses of Th. 1, the elastic rotatum p_e can be estimated via (9), where each component $\hat{u}_i$ of the unknown input $\hat{U}_k = (\hat{u}_1[k], \cdots, \hat{u}_n[k])^T$ is obtained by an i-th UIO whose state

$$\hat{X}_k^{(i)} = (\hat{x}_1^{(i)}[k], \hat{x}_2^{(i)}[k], \hat{x}_3^{(i)}[k])^T = (\hat{q}_i[k], \hat{\dot{q}}_i[k], \hat{\ddot{q}}_i[k])^T$$

is updated as

$$\begin{aligned} \hat{x}_j^{(i)}[k+1] &= \hat{x}_j^{(i)}[k] + T\,\hat{x}_{j+1}^{(i)}[k]\,, \text{ for } j = 1, 2\,, \\ \hat{x}_3^{(i)}[k+1] &= \frac{\alpha_1}{3}\beta[k] - \alpha_2\,\hat{x}_2^{(i)}[k] - 2\,\hat{x}_3^{(i)}[k]\,, \\ u_i[k] &= \alpha_3\beta[k] - \alpha_1\,\hat{x}_2^{(i)}[k] - \alpha_2\,\hat{x}_3^{(i)}[k]\,, \end{aligned} \tag{13}$$

with $\alpha_1 = \frac{3}{T^2}$, $\alpha_2 = \frac{3}{T}$, $\alpha_3 = \frac{1}{T^3}$, and $\beta[k] = q_i[k] - \hat{x}_1^{(i)}[k]$.

Proof 2: Given the UIO described by (7) and (8), the change of coordinates obtained via the permutation matrix

$$P = (e_1, e_{1+n}, e_{1+2n}, \cdots, e_i, e_{i+n}, e_{i+2n}, \cdots, e_n, e_{2n}, e_{3n})\,,$$

where e_i is the i-th vector of the canonical basis, leads to the new state vector $Z = P\hat{X} = (\hat{q}_1, \hat{\dot{q}}_1, \hat{\ddot{q}}_1, \cdots, \hat{q}_n, \hat{\dot{q}}_n, \hat{\ddot{q}}_n)^T$. The UIO dynamics in the new coordinates reads

$$Z_{k+1} = E'\,Z_k + F'\,\mathbb{Y}_k\,,\;\; \hat{U}_k = \mathcal{J}'\begin{pmatrix} Z_{k+1} - A'Z_k \\ q[k] - \hat{q}[k] \end{pmatrix}\,,$$

where $E' = PEP^T$, $A' = PA_nP^T$, matrix F' can be found by imposing

$$PF\mathbb{Y}_k = \begin{pmatrix} 0 & 0 & \frac{1}{T^2}\,q_1[k] & \cdots & 0 & 0 & \frac{1}{T^2}\,q_n[k] \end{pmatrix}^T = F'\mathbb{Y}_k$$

and matrix $\mathcal{J}'$ via the following steps:

$$\begin{aligned} \hat{U}_k &= \mathcal{J}\begin{pmatrix} \hat{X}_{k+1} - A_n\hat{X}_k \\ q[k] - \hat{q}[k] \end{pmatrix} = \mathcal{J}\begin{pmatrix} P^TZ_{k+1} - A_n\,P^TZ_k \\ q[k] - \hat{q}[k] \end{pmatrix} \\ &= \mathcal{J}\begin{pmatrix} P^T & 0_{3n,n} \\ 0_{n,3n} & \mathbb{I}_n \end{pmatrix}\begin{pmatrix} Z_{k+1} - PA_n\,P^TZ_k \\ q[k] - \hat{q}[k] \end{pmatrix} = \\ &= \mathcal{J}'\begin{pmatrix} Z_{k+1} - A'Z_k \\ q[k] - \hat{q}[k] \end{pmatrix}\,. \end{aligned}$$

It is straightforward to verify, via direct calculation, that the following block-diagonal matrices are obtained: $E' = \mathrm{diag}(\mathrm{E}_1, \cdots, \mathrm{E}_n)$, $\mathrm{F}' = \mathrm{diag}(\mathrm{F}_1, \cdots, \mathrm{F}_n)$, $\mathcal{J}' = \mathrm{diag}(\mathcal{J}_1, \cdots, \mathcal{J}_n)$, $\mathrm{A}' = \mathrm{diag}(\mathrm{A}'_1, \cdots, \mathrm{A}'_n)$, where $E_i = \bar{E}$, $F_i = \bar{F}$, $\mathcal{J}_i = \bar{\mathcal{J}}$, $A'_i = \bar{A}$, and

$$\bar{E} = \begin{pmatrix} 1 & T & 0 \\ 0 & 1 & T \\ -1/T^2 & -3/T & -2 \end{pmatrix},\; \bar{A} = \begin{pmatrix} 1 & T & 0 \\ 0 & 1 & T \\ 0 & 0 & 1 \end{pmatrix},$$
$$\bar{F} = \begin{pmatrix} 0_{2,3} & 0_{2,1} \\ 0_{1,3} & 1/T^2 \end{pmatrix},\; \bar{\mathcal{J}} = \begin{pmatrix} 0 & 0 & \frac{1}{T} & 0 \end{pmatrix}. \tag{14}$$

The block-diagonal form above shows that the UIO consists of n independent subsystems all described by the matrices $\bar{E}$, $\bar{F}$, $\bar{\mathcal{J}}$, and $\bar{A}$. The i-th subsystem state, $\hat{X}_k^{(i)}$, contains the i-th link position, speed, and acceleration estimates, i.e. $\hat{X}_k^{(i)} = (\hat{q}_i[k], \hat{\dot{q}}_i[k], \hat{\ddot{q}}_i[k])^T$. Renaming the subsystem state components as $\hat{x}_1^{(i)}$, $\hat{x}_2^{(i)}$, and $\hat{x}_3^{(i)}$, and expanding the state form expressions yield the decentralized rule in (13).

2) Stiffness Matrix Estimation: Since joints are elastically-decoupled, once the i-th elastic rotatum component, p_{e_i}, has been computed, the i-th diagonal entry of the joint stiffness matrix can be reconstructed by leveraging on the relations described in Tab. II. It can be seen that the i-th elastic rotatum and joint stiffness expressions are connected through the same coefficient vector Π_i, which is however unknown.

A strategy to find it is to use the i-th sequence of reconstructed elastic rotatum, $\{\hat{p}_{e_i}\}_k$, for $k = 0, 1, \cdots$, and minimize the approximation error between it and a regressor-based approximation of the form $\hat{p}_{e_i} = \Psi_i\,\hat{\Pi}_i$, where the specific regressor and coefficient vector expressions depend on the actuation principle as follows:

$$\begin{aligned} \Psi_{i,\mathrm{SEA}} &= \dot{\phi}_i, \hat{\Pi}_{i,\mathrm{SEA}} = \hat{\pi}_i\,, \\ \Psi_{i,\mathrm{sVSA}} &= \left((\mathcal{M}_{\kappa_\phi - 1} \otimes \mathcal{N}_{\kappa_{\theta_c}})\,\dot{\phi}_i, (\mathcal{M}_{\kappa_\phi} \otimes \mathcal{N}_{\kappa_{\theta_c} - 1})\,\dot{\theta}_{c_i}\right)\,, \\ \hat{\Pi}_{i,\mathrm{sVSA}} &= \begin{pmatrix} \hat{\Pi}_{\phi_i} \\ \hat{\Pi}_{\theta_{c_i}} \end{pmatrix} = \begin{pmatrix} (\mathcal{M}_{\kappa_\phi,\pi} \otimes \mathcal{N}^\tau_{\kappa_{\theta_c},\pi})^T \\ (\mathcal{M}^\tau_{\kappa_\phi,\pi} \otimes \mathcal{N}_{\kappa_{\theta_c},\pi})^T \end{pmatrix} \\ \Psi_{i,\mathrm{aVSA}} &= \left((1, \phi_{a_i}, \cdots, \phi_{a_i}^{\kappa-1})\,\dot{\phi}_{a_i}, (1, \phi_{b_i}, \cdots, \phi_{b_i}^{\kappa-1})\,\dot{\phi}_{b_i}\right)\,, \\ \hat{\Pi}_{i,\mathrm{aVSA}} &= (\hat{\pi}_{1,a_i}, \cdots, \hat{\pi}_{\kappa,a_i}, \hat{\pi}_{1,b_i}, \cdots, \hat{\pi}_{\kappa,b_i})^T\,, \end{aligned}$$

$$\begin{aligned} &\text{with } \mathcal{M}_\alpha = (1, \phi_i, \cdots, \phi_i^\alpha)\,,\; \mathcal{N}_\alpha = (1, \theta_{c_i}, \cdots, \theta_{c_i}^\alpha)\,, \\ &\mathcal{M}_{\alpha,\pi} = (\pi_{1,\phi_i}, \cdots, \pi_{\alpha,\phi_i})\,,\; \mathcal{N}_{\alpha,\pi} = (\pi_{1,\theta_{c_i}}, \cdots, \pi_{\alpha,\theta_{c_i}})\,, \\ &\mathcal{M}^\tau_{\alpha,\pi} = (\pi^\tau_{1,\phi_i}, \cdots, \pi^\tau_{\alpha,\phi_i})\,,\; \mathcal{N}^\tau_{\alpha,\pi} = (\pi^\tau_{1,\theta_{c_i}}, \cdots, \pi^\tau_{\alpha,\theta_{c_i}})\,. \end{aligned}$$

Afterward, once an estimate $\hat{\Pi}_i$ of the coefficient vector Π_i is iteratively obtained via the RLS, the i-th component of the joint stiffness can be estimated as $\hat{\sigma}_i[k] = \Phi_i\,\hat{\Pi}^\sigma_i[k]$, where

$$\begin{aligned} &\Phi_{i,\mathrm{SEA}} = 1, \hat{\Pi}^\sigma_{i,\mathrm{SEA}} = \hat{\Pi}_{i,\mathrm{SEA}}\,, \\ &\Phi_{i,\mathrm{sVSA}} = \mathcal{M}_{\kappa_\phi - 1} \otimes \mathcal{N}_{\kappa_{\theta_c}}\,, \hat{\Pi}^\sigma_{i,\mathrm{sVSA}} = \hat{\Pi}_{\phi_i}\,, \\ &\Phi_{i,\mathrm{aVSA}} = \left(1, \cdots, \phi_{a_i}^{\kappa-1}, 1, \cdots, \phi_{b_i}^{\kappa-1}\right), \hat{\Pi}^\sigma_{i,\mathrm{aVSA}} = \hat{\Pi}_{i,\mathrm{aVSA}}. \end{aligned}$$

Remark 1: The UIO uses only the robot's link positions

SEA	$\tau_{e_i} = \pi_i\,\phi_i, \quad p_{e_i} = \pi_i\,\dot{\phi}_i\,, \quad \sigma_i = \pi_i\,,$
sVSA	$\tau_{e_i} \approx \sum_{j=0}^{\kappa_\phi} \pi^\tau_{j,\phi_i}\,\phi_i^j \sum_{j=0}^{\kappa_{\theta_c}} \pi^\tau_{j,\theta_{c_i}}\,\theta_{c_i}^j\,,$ $p_{e_i} \approx \left(\sum_{j=1}^{\kappa_\phi} \pi_{j,\phi_i}\,\phi_i^{j-1}\right)\left(\sum_{j=1}^{\kappa_{\theta_c}} \pi^\tau_{j,\theta_{c_i}}\,\theta_{c_i}^j\right)\dot{\phi}_i +$ $+ \left(\sum_{j=1}^{\kappa_\phi} \pi^\tau_{j,\phi_i}\,\phi_i^j\right)\left(\sum_{j=1}^{\kappa_{\theta_c}} \pi_{j,\theta_{c_i}}\,\theta_{c_i}^{j-1}\right)\dot{\theta}_{c_i}\,,$ $\sigma_i \approx \left(\sum_{j=1}^{\kappa_\phi} \pi_{j,\phi_i}\,\phi_i^{j-1}\right)\left(\sum_{j=1}^{\kappa_{\theta_c}} \pi^\tau_{j,\theta_{c_i}}\,\theta_{c_i}^j\right)\,,$
aVSA	$\tau_{e_i} \approx \sum_{j=0}^{\kappa} \pi^\tau_{j,a_i}\,\phi_{a_i}^j + \sum_{j=0}^{\kappa} \pi^\tau_{j,b_i}\,\phi_{b_i}^j\,,$ $p_{e_i} \approx \left(\sum_{j=1}^{\kappa} \pi_{j,a_i}\,\phi_{a_i}^{j-1}\right)\dot{\phi}_{a_i} + \left(\sum_{j=1}^{\kappa} \pi_{j,b_i}\,\phi_{b_i}^{j-1}\right)\dot{\phi}_{b_i}\,,$ $\sigma_i \approx \sum_{j=1}^{\kappa} \pi_{j,a_i}\,\phi_{a_i}^{j-1} + \sum_{j=1}^{\kappa} \pi_{j,b_i}\,\phi_{b_i}^{j-1}\,.$

TABLE II
APPROXIMATION FUNCTIONS OF ELASTIC TORQUE τ_{e_i}, ELASTIC ROTATUM p_{e_i} AND JOINT STIFFNESS σ_i FOR EACH ACTUATION PRINCIPLES. FOR SVSA AND AVSA, IT STANDS THAT $\pi_j = j\,\pi^\tau_j$.

and leans on the knowledge of inertia matrix, Coriolis and centrifugal terms, and gravity vector, but neither force/torque sensor nor control input signal are required. The RLS filter uses motor positions and speeds to estimate stiffness.

Remark 2 (Cartesian stiffness): While we focus here on estimating the joint stiffness matrix σ, it is worth connecting it to the stiffness σ_c in the Cartesian task-space. Assume for simplicity that the interaction with the environment occurs at the robot's tip through a constant Cartesian force $\bar{f}_{\text{ext}} = J(q)^{-T}\bar{\tau}_{\text{ext}}$, and that the robot itself is at a point $\bar{q}$ satisfying the equilibrium condition $\bar{\tau}_e = J(\bar{q})^T\bar{f}_{\text{ext}} - G(\bar{q})$, where $\bar{\tau}_e$ is a constant elastic torque and J is the robot's Jacobian matrix, assumed to be square and invertible without loosing the generality. Along the lines of [24], suppose that the system is perturbed by variations $\delta\tau_e$ and δf_{ext} of the elastic torque and external Cartesian force, respectively, and that a new nearby equilibrium $q = \bar{q} + \delta q$ is reached. Taylor's expansion to the first-order of the new equilibrium condition gives, $\bar{\tau}_e + \delta\tau_e = J(\bar{q}+\delta q)^T(\bar{f}_{\text{ext}} + \delta f_{\text{ext}}) - G(\bar{q}+\delta q)$ and then $\delta\tau_e = \left(J_q(\bar{q})^T\bar{f}_{\text{ext}} - G_q(\bar{q})\right)J(\bar{q})^{-1}\delta x + J(\bar{q})^T\,\delta f_{\text{ext}}$, where $J_q(\bar{q}) = \frac{\partial J(q)}{\partial q}|_{q=\bar{q}}$, $G_q(\bar{q}) = \frac{\partial G(q)}{\partial q}|_{q=\bar{q}}$ and the relation $\delta x = J(\bar{q})\,\delta q$ for the tip position variation is used. By the joint stiffness definition, $\delta\tau_e = \sigma(\bar{q})\,\delta q = \sigma(\bar{q})\,J(\bar{q})^{-1}\delta x$, and the Cartesian stiffness definition, $\delta f_{\text{ext}} = \sigma_c\,\delta x$, one finally gets $\sigma_c = J(\bar{q})^{-T}\left(\sigma(\bar{q}) - J_q(\bar{q})^T\bar{f}_{\text{ext}} + G_q(\bar{q})\right)J(\bar{q})^{-1}$. The value $\bar{f}_{\text{ext}}$, needed to evaluate the formula, can be found using force/torque sensors mounted at the tip or retrieved via virtual sensors [25]. Moreover, since the considered articulated soft robots have elastically decoupled joints, σ is diagonal and hence symmetric by construction. Yet, the stiffness in the task space may include an asymmetric part, $\sigma_a = \frac{1}{2}(\sigma_c - \sigma_c^T)$, whose importance is discussed in [26].

Remark 3 (Choice of T): The ability to deal with tasks where stiffness is dynamically changing is connected to the sampling period T. After the initial transient where the RLS learns the stiffness model parameters, the only estimation delay is of the $L = 3$ samples or, equivalently, $3T$ seconds due to the UIO (Th. 1). Thus, the frequency range for tasks that are manageable by the solution reaches $f = \frac{1}{3T}$ Hz. For instance, if $T = 5\cdot10^{-3}$ seconds, $f = 67$ Hz.

Remark 4 (Model uncertainty): Compared to fully sensor-based approaches, this method relies on accurate knowledge of the system model. When only incomplete knowledge is available, the achieved performance reduces. Unmeasured external force/torque, non-negligible friction, and parametric uncertainty lead to the perturbed elastic rotatum estimate, $\hat{p}_e^*[k] = \hat{p}_e[k] - \frac{d}{dt}\left(J^T(q)f_{\text{ext}} - \gamma(\dot{q}) - Y(q,\dot{q},\ddot{q})\,\tilde{\pi}\right)$, where $\tilde{\pi}$ depends on the parametric uncertainty and Y is a suitable regressor, and, hence, yield bounded but non-zero steady-state error in the estimated joint stiffness. Here, traditional system identification methods used to mitigate the model uncertainties are not an immediate solution because precise torque/current measurement is required [27]. A qualitative strategy to evaluate the impact of uncertainty is obtained by assuming that the robot tracks a trajectory $q_d(t)$ while also an unmodeled friction $\gamma(\dot{q}) = \mu_s\text{sgn}(\dot{q}) + \mu_v\dot{q}$ acts. In this case, (10) becomes $M(q_d)\,q_d^{(3)} + \dot{M}(q_d)\,\ddot{q}_d + \dot{C}(q_d,\dot{q}_d)\,\dot{q}_d + C(q_d,\dot{q}_d)\ddot{q}_d + \dot{G}(q_d,\dot{q}_d) + p_e + \dot{\gamma}(\ddot{q}_d) = 0$. If $q_d(t)$ contains frequencies up to 1 $\frac{\text{rad}}{\text{s}}$, its time derivatives have progressively smaller amplitudes; so, uncertain parameters multiplying higher derivatives have less impact. Similar reasoning stands for viscous friction, while static friction can be handled by *selective* RLS that stops the update when the link speed is close to a sign change. Quantization error introduced by encoders is filtered out by the RLS and is not an issue.

Remark 5 (Computational complexity): The approach scales linearly with n on a single-processing machine and sub-linearly on the paralleled one. Indeed, computing $\hat{U}_k$ requires n independent executions of the 1-DoF UIO described in Corollary 1, whose complexity is $\mathcal{O}(1)$; evaluating $\hat{p}_e[k]$ in (9) amounts to computing the robot's inverse dynamics whose complexity is $\mathcal{O}(n)$ or $\mathcal{O}(\log_2 n)$ for single or paralleled units; finally, estimating σ_k requires n independent executions of a 1-DoF RLS whose complexity depends on the involved polynomials and is $\mathcal{O}(\eta^2)$ with $\eta = 1$ for SEA, $\eta = \kappa_\phi\kappa_{\theta_c}$ for sVSA, and $\eta = \kappa$ for aVSA. Hence, the total complexity is $\mathcal{O}(n{+}n{+}n\eta^2) = \mathcal{O}(n\eta^2)$ on a single and $\mathcal{O}(1{+}\log_2 n{+}\eta^2) = \mathcal{O}(\log_2 n + \eta^2)$ on a paralleled machine. To exemplify, on a single-process machine with 1.8GHz, the computation times are always below 1 ms, which ensures method's real-time applicability.

IV. Simulation results

Herein, we show the solution's effectiveness in simulation with a 1-DoF articulated soft robot that is actuated, alternatively, by a SEA, an sVSA, or an aVSA and then show the sensitivity of the solution to various uncertainties on a 2-DoF robot actuated by aVSA. The stiffness estimator is obtained by designing a UIO as in Th. 1 for 1-DoF and an RLS filter as described in [14]. Precisely, the former reconstructs the elastic rotatum signal p_{e_1}, and the latter finds the sought link stiffness signal σ_1. In all three cases, the robot link position follows a sinusoidal trajectory. Effectiveness of the results is assessed by using the Mean Square Error (MSE) and Mean Square Relative Error Percentage (MSREP) indices,

$$\text{MSE} = \tfrac{1}{n_2-n_1+1}\textstyle\sum_{n=n_1}^{n_2}(\chi(n) - \hat{\chi}(n))^2\,,$$
$$\text{MSREP} = \tfrac{1}{n_2-n_1+1}\textstyle\sum_{n=n_1}^{n_2}\left(\chi(n) - \hat{\chi}(n)\right)^2/\chi^2(n)\,,$$

where χ indicates the real quantity, $\hat{\chi}$ the estimated one, n_1 and n_2 the initial and final times. For all simulations the time interval is $t \in [20, 100]$ s. In the figures, the ordinate's labels are placed within the sub-figure titles, and the time axis is shared for all subfigures in the same column for compactness.

A. Series elastic actuation

We adopt here a series elastic actuator with a spring constant $K = 103$ Nm/rad [28]. The elastic torque, elastic rotatum, and joint stiffness expressions for this actuator are given by $\tau_{e_1} = K(q_1 - \theta_1)$, $p_{e_1} = K(\dot{q}_1 - \dot{\theta}_1)$, and $\sigma_1 = K$, respectively. As in Sec. III-B, the elastic rotatum p_{e_1} is first reconstructed by a UIO, and afterwards, the unknown parameter π_1, also representing the sought stiffness σ_1, is estimated via an RLS based on the equation $\hat{p}_{e_1} = \dot{\phi}_1\hat{\pi}_1$. As no a-priori information on the stiffness value is used, the RLS filter is initialized with an estimate and a covariance matrix being $\hat{\pi}_1[0] = 0$ and $P[0] = 10^7$. The stiffness estimation results are depicted in the leftmost part of Fig. 2, showing that the solution manages to learn precisely the value of σ_1, which is in line with the performance indices $\text{MSE} = 2.2{\cdot}10^{-4}\ \frac{\text{N}^2\text{m}^2}{\text{rad}^2}$ and $\text{MSREP} = 2.1\cdot10^{-6}$ %.

B. Serial variable stiffness actuation

To illustrate the stiffness estimation performance for sVSA type of actuators, we choose herein the actuator AwAS [17],

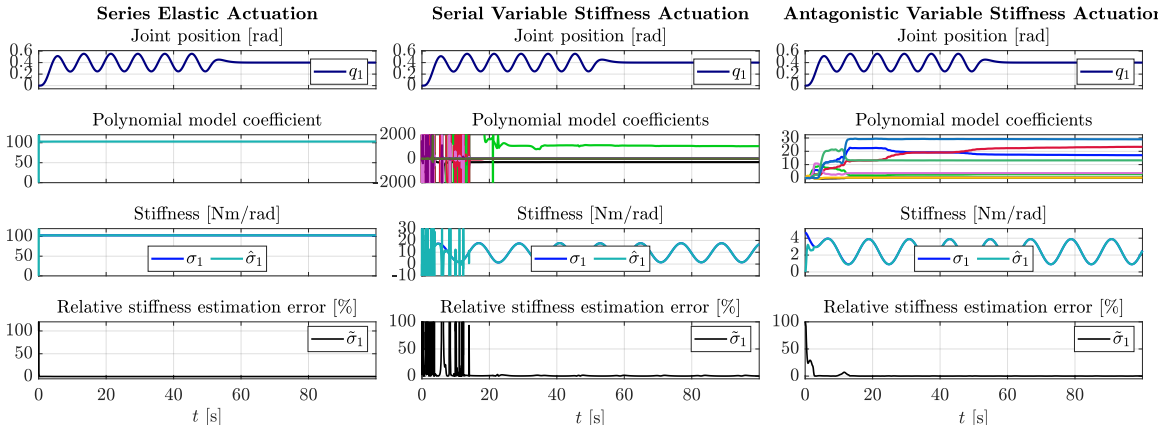

Fig. 2. Simulation #1 (1-DoF articulated soft robot actuated by SEA, sVSA and aVSA mechanisms) - From top to bottom, position of the robot link q_1, temporal evolution of the RLS parameters vector, real stiffness σ_1 and estimated stiffness $\hat{\sigma}_1$, and the corresponding relative estimation error w.r.t the stiffness model, i.e. $\tilde{\sigma}_1 = |\sigma_1 - \hat{\sigma}_1|/\sigma_1$. After an initial period, the stiffness is accurately estimated with small relative error, with the RLS parameters converging and then remaining constant. In case of SEA-driven robots, RLS parameter has a physical meaning of SEA spring constant that is also a joint stiffness, while for sVSA and aVSA-driven robots, RLS parameters determine the coefficients of elastic rotatum and joint stiffness polynomial models.

whose elastic torque, elastic rotatum, and stiffness functions are defined as: $\tau_{e_1} = k_s(r_0 - b\theta_{c_1})^2 \sin 2\phi_1$, $p_{e_1} = 2k_s(r_0 - b\theta_{c_1})^2 \cos 2\phi_1 \, \dot{\phi}_1 - 2k_s b(r_0 - b\theta_{c_1}) \sin 2\phi_1 \, \dot{\theta}_{c_1}$, $\sigma_1 = 2k_s(r_0 - b\theta_{c_1})^2 \cos 2\phi_1$, where k_s is the spring constant, r_0 is the initial lever arm length, and b is transmission ratio between the second motor and the ball screw.

We start with the assumption that initial value of parameters is null, i.e. $\hat{\Pi}_{\phi_1}[0] = 0_{6,1}$ and $\hat{\Pi}_{\theta_{c_1}}[0] = 0_{4,1}$ and that the covariance matrix is $P[0] = 10^7$. The Taylor expansion of elastic rotatum comprises terms obtained for $\kappa_\phi = 3$ and $\kappa_{\theta_c} = 2$. Only even powers of ϕ_1 have been considered since the function to be approximated is even with respect to it. The simulation outcome is shown in the middle part of Fig. 2, where it is easily observed that the estimator successfully picks up the stiffness information. Indices $\text{MSE} = 1.5 \cdot 10^{-3} \ \frac{\text{N}^2\text{m}^2}{\text{rad}^2}$ and $\text{MSREP} = 6 \cdot 10^{-3} \ \%$ show the good performance also from the numerical perspective.

C. Antagonistic variable stiffness actuation

Adopting, as an example, the commercially available aVSA, *qbmove*, the elastic torque, elastic rotatum, and joint stiffness functions are $\tau_{e_1} = k \sinh(a\phi_{a_1}) + k \sinh(a\phi_{b_1})$, $p_{e_1} = a\,k \cosh(a\phi_{a_1}) \, \dot{\phi}_{a_1} + a\,k \cosh(a\phi_{b_1}) \, \dot{\phi}_{b_1}$, $\sigma_1 = a\,k \cosh(a\phi_{a_1}) + a\,k \cosh(a\phi_{b_1})$, where $\phi_{a_1} = q_1 - \theta_{a_1}$, $\phi_{b_1} = q_1 - \theta_{b_1}$, and where k and a are spring constants of suitable values [22]. The RLS is based on a 6-th order Taylor expansion of the elastic rotatum expression. Only even powers of ϕ_{a_1} and ϕ_{b_1} are considered since the function to be approximated is even. Complete lack of knowledge of Π_1 is assumed, i.e. $\hat{\Pi}_1[0] = 0_{8,1}$ and $P_1[0] = 10^7$. Fig. 2 rightmost part shows the simulation results and reveals that, after an initial transient, the joint stiffness is successfully tracked over time. Specifically, indices MSE and MSREP result in $1 \cdot 10^{-4} \ \frac{\text{N}^2\text{m}^2}{\text{rad}^2}$ and $3.4 \cdot 10^{-4} \ \%$, respectively.

Finally, we illustrate Remark 4 in Fig. 3 by showing the influence of parametric and structural model uncertainties on a 2-DoF setup of robot driven by aVSA qbmove actuators. A parametric deviation of 20% from nominal values is considered and $q_d(t)$ is set to change with frequency of $\frac{\pi}{6} \frac{\text{rad}}{\text{s}}$.

V. Experimental results

We now move on to the experimental validation of our method with real articulated soft robots actuated by *qbmove* aVSA devices. The Reader may refer to [22] for a detailed description of these actuators. We first characterize the elastic torque and stiffness models for each actuator used, to obtain ground-truth information. Then, we proceed with testing the UIO+RLS-based solution on the real robots with different configurations, when the robot is moving and when it is in co-contraction mode, i.e. when only the joint stiffness is changing while the joint position is still.

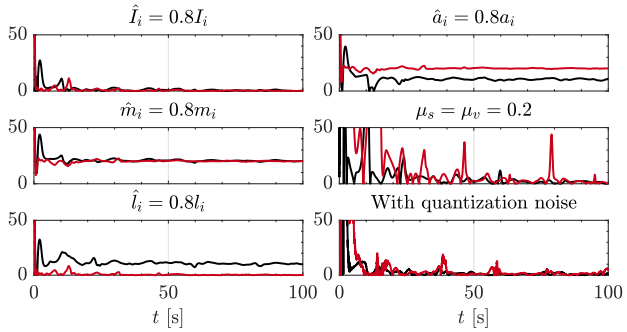

Fig. 3. Relative stiffness estimation errors in percentage due to uncertainty for a 2-DoF robot actuated by aVSA. The graphs separately report the effect of a 20% deviation of links' inertia, mass, length, and center of mass and presence of static and viscous friction ($\mu_s = \mu_v = 0.2$). The quantization noise mimics an encoder with the resolution of $2 \cdot 10^{-4}$ rad. Black and red lines refer to 1^{st} and 2^{nd} joints' stiffness. Plots show that the estimation is stable and that inertia has the least effect since it multiplies the jerk (10).

A. Stiffness Characterization

A characterization of the *qbmove* actuators is carried out according to the procedure described in [29]. First, the data needed for the characterization is acquired. To this aim, an ATI Axia80-M20 torque sensor has been installed on the shaft of each VSA, to record ground-truth values of the actual elastic torque. Synchronized measures of motor and link positions along with the applied torque are repeatedly collected for stiffness presets ranging from 0% to 100%.

Next, we derive a fitted model for the elastic torque. We adopt here a method that consists of obtaining an analytical model of the elastic torque and then symbolically differentiating it in the deflection. Following the suggestion from the datasheet, we have chosen to use the following reference model for the elastic torque: $\mathcal{T}_{e,i} = k_i \sinh(a_i(q_i - \theta_{a_i})) + k_i \sinh(a_i(q_i - \theta_{b_i}))$, where a_i and k_i are spring constants to be learnt, while q_i, θ_{a_i}, and θ_{b_i} are the independent variables.

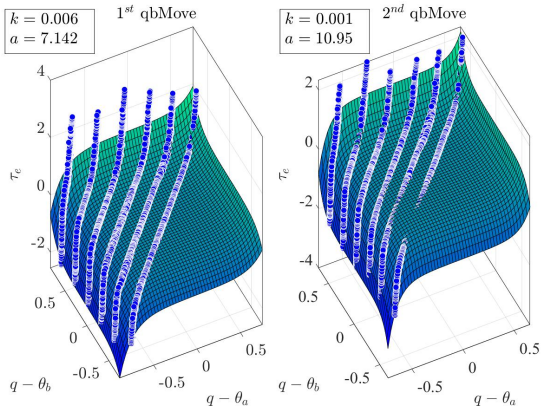

Fig. 4. Graphical representations of the fitting functions $\mathcal{T}_{e,i}$ for the elastic torque models of the two used qbmove actuators.

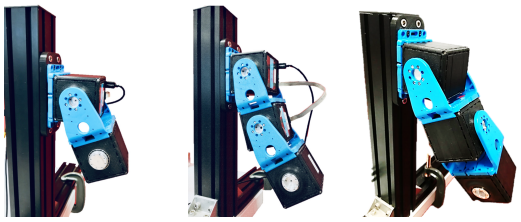

Fig. 5. The three hardware setups used to validate the proposed approach. From left to right: a 1-DoF setup; a 2-DoF setup on the vertical plane ("A") with DH parameters $(a_i, \alpha_i, d_i, \theta_i) = \{(l, 0, 0, q_1), (l, 0, 0, q_2)\}$ where l is the link length; and a 2-DoF setup in the 3D space ("B") with DH parameters $(a_i, \alpha_i, d_i, \theta_i) = \{(l, -\frac{\pi}{2}, 0, q_1), (l, 0, 0, q_2)\}$. In all configurations, the last actuator in the chain is passive and acts as a load.

They comprise *qbmove Maker Pro* VSAs that are connected via rigid links.

The estimator is implemented in Matlab/Simulink and the link and motor positions are acquired with a sampling period $T = 5 \cdot 10^{-3}$ seconds by using software library blocks provided by the manufacturer.

The results of fitting the data are shown in Fig. 4. Finally, by applying the Trust-Region-Reflective fitting algorithm, a confidence interval for the validity of the obtained function is calculated. Given the elastic torque samples, $\bar{\tau}_{e,i}^{(j)}$, for $j = 1, \cdots, N$, where N is the number of samples, collected for all stiffness presets, one convenient way to quantify this interval is to calculate the Root Mean Square Relative error c_i between the samples and the fitted function $\mathcal{T}_{e,i}$. In formula we have $c_i = \sqrt{\frac{1}{N}\sum_{j=1}^{N}(\bar{\tau}_{e,i}^{(j)} - \mathcal{T}_{e,i})^2/(\bar{\tau}_{e,i}^{(j)})^2}, 100\ \%$. The interpretation of the confidence interval is that all values that differ, in absolute sense, from the nominal value of $\mathcal{T}_{e,i}$ of at most the root mean square relative error are to be considered correct. In closing, the experimental data used to fit the elastic torque models of the two *qbmove* actuators leads to the functions illustrated in Fig. 4, that have confidence intervals $c_1 = 19.96\ \%$ and $c_2 = 21.06\ \%$. For simplicity, they are rounded to $c_i = 20\ \%$ in the remainder. The hypothesis we make here is that the same interval is translated to the stiffness model [6]. Thus, stiffness estimation errors below 20 % will be considered as satisfactory.

B. Validation of the proposed stiffness estimation approach

The hardware setups used for the validation are illustrated in Fig. 5. The approach is first validated on a 1-DoF setup, which is the leftmost hardware setup in Fig. 5. The robot's mass, inertia, and link length are $m = 0.26$ kg, $I = 2.1 \cdot 10^{-3}$ kgm^2, and

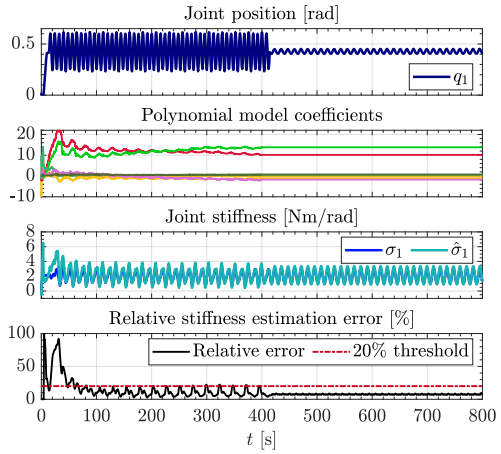

Fig. 6. Experiment #1 (1-DoF setup) - The figure shows the link position, the learned RLS parameters, the real and estimated stiffness, and finally the relative estimation error. For $t \in [0, 420]$, the robot's position and stiffness are both moving. After an initial transient during which the RLS algorithm learns appropriate values for Taylor coefficients, the joint stiffness relative estimation error $|\sigma_1 - \hat{\sigma}_1|/\sigma_1$ nicely converges to within a threshold of 20% from the nominal value, which is consistent with the confidence interval c_1 of the first actuator. During the first phase (and more precisely after the convergence of the RLS parameters, i.e. for $t \in [150, 420]$), the indices MSE and MSREP amount to 0.23 N^{2}m^2/rad^2 and 0.71%, respectively.
Subsequently, for $t \in (420, 800]$, the robot is required to have a co-contraction behavior for two purposes: first to show that our method does not suffer from observability issues, even when the robot position is steady [9], and then to display the RLS performance even under fewer excitation. The experiment shows that a simple algorithmic modification, where the RLS parameters' update is temporarily stopped, whenever the robot's position becomes steady, allows maintaining the estimation error below the confidence interval threshold. During this second phase, the MSE and MSREP coefficients lower down to 0.06 N^{2}m^2/rad^2 and 0.26%.

$l = 0.09$ m. The Taylor coefficients of the elastic rotatum and stiffness are assumed to be fully unknown, which is obtained by choosing null initial values for the RLS parameters, i.e. $\Pi_1[0] = 0_{8,1}$, and an initial covariance matrix $P_1[0] = 10^2$. As in the simulation part, since the elastic rotatum and the stiffness are even functions, the regressor only uses even powers of the deflections up to the sixth order. The experiment details are reported in Fig. 6.

Let us now proceed with testing the multi-DoF stiffness estimator on a real 2-DoF soft robot in two different configurations (see the middle and the rightmost setup in Fig. 5). It can be observed that, due to the coupled terms in the robot's dynamics, the present test represents a greater challenge for the noninvasive stiffness estimation. The inertia, mass, and length parameters of both links are equivalent and have the same values as provided in the previous paragraph. The obtained estimator consists of two identical copies of the UIO, as in Corollary 1, and the same number of instances of the RLS algorithm. Again, complete lack of knowledge about Taylor expansions' coefficients of the elastic rotatum and stiffness functions is assumed. Consequently, both RLS algorithms are initialized with parameter vectors $\Pi_1[0] = \Pi_2[0] = 0_{8,1}$ and covariance matrices $P_1[0] = P_2[0] = 10^4$.

The results obtained during the test with the two configurations are reported in Fig. 7 and Fig. 8. Despite the simultaneous motions of position and stiffness for both links, and the different configurations, the proposed approach can accurately estimate the joints' stiffness within the confidence intervals of the two *qbmove* actuators, c_1 and c_2. After an initial transient, the two RLS learn proper Taylor coefficients and accurately track the real stiffness.

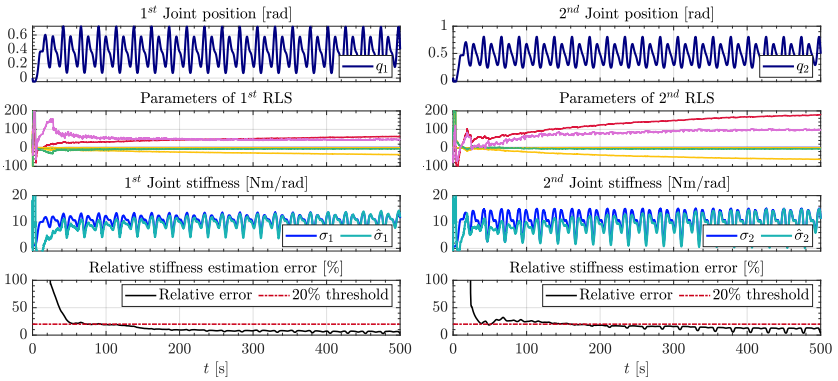

Fig. 7. Experiment #2 (2-DoF "A" setup). After an initial transient when Taylor's coefficients are learned, the joint stiffness estimation errors, $|\sigma_i - \hat{\sigma}_i|/\sigma_i$, smoothly converge to within the 20%-threshold from the nominal value. The decentralized UIO+RLS-based solution successfully estimates the sought signal. The obtained performance indices, MSE and MSREP, evaluated after the transient ($t \in (300, 500]$), are, for the first joint, 0.5 $\mathrm{N^2m^2/rad^2}$ and 1 % and, for the second one, 0.8 $\mathrm{N^2m^2/rad^2}$ and 4.8 %, respectively.

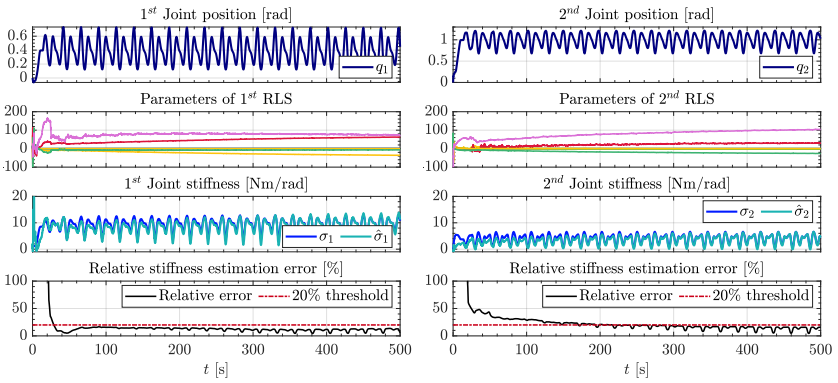

Fig. 8. Experiment #3 (2-DoF "B" setup). After an initial transient when Taylor's coefficients are learned, the joint stiffness estimation errors, $|\sigma_i - \hat{\sigma}_i|/\sigma_i$, smoothly converge to within the 20%-threshold from the nominal value. The decentralized UIO+RLS-based solution successfully estimates the sought signal. The obtained performance indices, MSE and MSREP, evaluated after the transient ($t \in (300, 500]$), are, for the first joint, 0.9 $\mathrm{N^2m^2/rad^2}$ and 3.6 % and, for the second one, 0.1 $\mathrm{N^2m^2/rad^2}$ and 7.1 %, respectively.

VI. Conclusion

A new approach to stiffness estimation in articulated soft robots was introduced, which needs no a-priori knowledge of the actuation model parameters and uses only motor states, link position, and dynamics. Its validation was done with multi-DoF configurations, different actuator types, in simulation and with experiments. Results confirmed accurate estimation even when the robot is co-contracting. An important benefit, confirmed by the experiments, is the avoidance of installing force/torque sensors. Future work will expand the approach to estimate Cartesian stiffness and deal with possible environment interaction, model uncertainty, and measurement noise.

References

[1] A. De Luca and W. Book, "Robots with flexible elements," in *Handbook of robotics*, B. Siciliano and O. Khatib, Eds. Springer, 2016, ch. 11.

[2] A. Albu-Schäffer and A. Bicchi, "Actuators for soft robotics," in *Handbook of robotics*, B. Siciliano and O. Khatib, Eds. Springer, 2016, ch. 21, pp. 243–282.

[3] M. Ruderman, T. Bertram, and M. Iwasaki, "Modeling, observation, and control of hysteresis torsion in elastic robot joints," *Mechatronics*, vol. 24, no. 5, pp. 407–415, 2014.

[4] N. Diolaiti, C. Melchiorri, and S. Stramigioli, "Contact impedance estimation for robotic systems," *Trans. Robot.*, vol. 21, no. 5, pp. 925–935, 2005.

[5] F. Flacco *et al.*, "On-line estimation of variable stiffness in flexible robot joints," *Int. J. Rob. Res.*, vol. 31, no. 13, pp. 1556–1577, 2012.

[6] T. Ménard, G. Grioli, and A. Bicchi, "A stiffness estimator for agonistic–antagonistic variable-stiffness-actuator devices," *Trans. Robot.*, vol. 30, no. 5, pp. 1269–1278, 2014.

[7] A. Fagiolini, M. Trumic, and K. Jovanovic, "An input observer-based stiffness estimation approach for flexible robot joints," *Robot. Autom. Lett.*, 2020.

[8] F. Flacco and A. De Luca, "Stiffness estimation and nonlinear control of robots with variable stiffness actuation," *IFAC Proc.*, vol. 44, no. 1, pp. 6872–6879, 2011.

[9] G. Grioli and A. Bicchi, "A non-invasive, real-time method for measuring variable stiffness," *Robotics Science and Systems VI*, 2010.

[11] Z. Li *et al.*, "Asymmetric bimanual control of dual-arm exoskeletons for human-cooperative manipulations," *Trans. Robot.*, vol. 34, no. 1, pp. 264–271, 2017.

[10] G. Grioli and A. Bicchi, "A real-time parametric stiffness observer for vsa devices," in *Int. Conf. Robot. and Autom.* IEEE, 2011, pp. 5535–5540.

[12] M. Howard, D. J. Braun, and S. Vijayakumar, "Transferring human impedance behavior to heterogeneous variable impedance actuators," *Trans. Robot.*, vol. 29, no. 4, pp. 847–862, 2013.

[13] S. Sundaram and C. N. Hadjicostis, "Partial state observers for linear systems with unknown inputs," *Automatica*, vol. 44, no. 12, pp. 3126–3132, 2008.

[14] L. Ljung, "System identification: theory for the user," *PTR Prentice Hall, Upper Saddle River, NJ*, pp. 1–14, 1999.

[15] F. Angelini *et al.*, "Online optimal impedance planning for legged robots," in *Int. Conf. Intell. Robots Syst.* IEEE, 2019, pp. 6028–6035.

[16] G. A. Pratt and M. M. Williamson, "Series elastic actuators," in *Int. Conf. Intell. Robots Syst.*, vol. 1. IEEE, 1995, pp. 399–406.

[17] A. Jafari *et al.*, "A novel actuator with adjustable stiffness (awas)," in *Int. Conf. Intel. Rob. Syst.* IEEE, 2010, pp. 4201–4206.

[18] J. Sun *et al.*, "Design, modeling and control of a novel compact, energy-efficient, and rotational serial variable stiffness actuator (svsa-ii)," *Mech. Mac. Theory*, vol. 130, pp. 123–136, 2018.

[19] S. S. Groothuis *et al.*, "The vsaut-ii: A novel rotational variable stiffness actuator," in *Int. Conf. Robot. and Autom.* IEEE, 2012, pp. 3355–3360.

[20] M. G. Catalano *et al.*, "Vsa-hd: From the enumeration analysis to the prototypical implementation," in *Int. Conf. Intell. Robots Syst.* IEEE, 2010, pp. 3676–3681.

[21] O. Eiberger *et al.*, "On joint design with intrinsic variable compliance: Derivation of the dlr qa-joint," in *Int. Conf. Robot. and Autom.* IEEE, 2010, pp. 1687–1694.

[22] "QbMove Maker Pro datasheet," https://www.qbrobotics.com.

[23] F. Flacco, "Modeling and control of robots with compliant actuation," *PhD thesis*, 2012.

[24] A. Ajoudani, N. G. Tsagarakis, and A. Bicchi, "Choosing poses for force and stiffness control," *IEEE Trans. on Robot.*, vol. 33, no. 6, pp. 1483–1490, 2017.

[25] L. Roveda *et al.*, "6d virtual sensor for wrench estimation in robotized interaction tasks exploiting extended kalman filter," *Machines*, vol. 8, no. 4, p. 67, 2020.

[26] N. Ciblak and H. Lipkin, "Asymmetric cartesian stiffness for the modelling of compliant robotic systems," in *Intl. Design Eng. Techn. Conf. and Comp. & Inform. in Eng. Conf.* ASME, 1994, pp. 197–204.

[27] J. Hollerbach, W. Khalil, and M. Gautier, "Model identification," in *Handbook of robotics*, B. Siciliano and O. Khatib, Eds. Springer, 2016, ch. 6.

[28] M. Laffranchi *et al.*, "Development and control of a series elastic actuator equipped with a semi active friction damper for human friendly robots," *Robot. Auton. Syst.*, vol. 62, no. 12, pp. 1827–1836, 2014.

[29] G. Grioli *et al.*, "Variable stiffness actuators: The user's point of view," *The Int. J. Rob. Res.*, vol. 34, no. 6, pp. 727–743, 2015.